Identification of Host Proteins Required for HIV Infection Through a Functional Genomic Screen

Abraham L. Brass, *et al.*

Science **319**, 921 (2008);
DOI: 10.1126/science.1152725

Science (print ISSN 0036-8075; online ISSN 1095-9203) is published weekly, except the last week in December, by the American Association for the Advancement of Science, 1200 New York Avenue NW, Washington, DC 20005.

Identification of Host Proteins Required for HIV Infection Through a Functional Genomic Screen

Abraham L. Brass,[1,2] Derek M. Dykxhoorn,[3*] Yair Benita,[4*] Nan Yan,[3] Alan Engelman,[5] Ramnik J. Xavier,[2,4] Judy Lieberman,[3] Stephen J. Elledge[1†]

HIV-1 exploits multiple host proteins during infection. We performed a large-scale small interfering RNA screen to identify host factors required by HIV-1 and identified more than 250 HIV-dependency factors (HDFs). These proteins participate in a broad array of cellular functions and implicate new pathways in the viral life cycle. Further analysis revealed previously unknown roles for retrograde Golgi transport proteins (Rab6 and Vps53) in viral entry, a karyopherin (TNPO3) in viral integration, and the Mediator complex (Med28) in viral transcription. Transcriptional analysis revealed that HDF genes were enriched for high expression in immune cells, suggesting that viruses evolve in host cells that optimally perform the functions required for their life cycle. This effort illustrates the power with which RNA interference and forward genetics can be used to expose the dependencies of human pathogens such as HIV, and in so doing identify potential targets for therapy.

HIV-1 encodes only 15 proteins (*1*) and thus must exploit multiple host cell functions for successful infection (*2*). Viral entry depends on binding to the receptor CD4 and either of two co-receptors, CXCR4 or CCR5. Upon membrane fusion, the viral core, containing the viral capsid and nucleocapsid along with the viral genome, reverse transcriptase (RT), integrase (IN), protease (PR), and the viral accessory proteins Vif, Nef, and Vpr, is released into the cytoplasm. Collectively called the reverse transcription complex (RTC), this assembly binds to actin, triggering the synthesis of a double-stranded viral DNA complement that forms the preintegration complex (PIC), which moves along microtubules to the nucleus and enters via a nuclear pore.

IN binds to host lens epithelium-derived growth factor (LEDGF) and catalyzes HIV DNA integration. Proviral transcription depends on the viral factor Tat, which binds to the transactivation response element (TAR) in the proviral RNA and promotes elongation by recruiting cyclin T1, HIV-1 Tat specific factor 1 (HTATSF1), and Cdk9. Unspliced and partially spliced HIV transcripts require the viral Rev protein for nuclear export. HIV buds directly from the plasma membrane through association with the host class E Vps proteins (*3*). Because of the complexity of the retroviral life cycle and the small number of viral proteins, important viral-host relationships likely remain to be discovered. Toward this goal, we performed a genome-wide RNA interference screen to identify host factors involved in HIV-1 infection.

The siRNA screen. We developed a two-part screen to detect host proteins needed for HIV infection (Fig. 1A) (*4*). Part one consisted of infecting small interfering RNA (siRNA)–transfected cells with the IIIB strain of HIV-1 [HIV-IIIB (*4*); SOM Text] and 48 hours later staining for p24, produced from the HIV *gag* gene. This screen detects host proteins needed from viral entry through Gag translation, but is less sensitive for factors affecting viral assembly and budding. To identify late-acting factors, we performed part two by incubating culture supernatants from part one with fresh reporter cells and assaying for Tat-dependent reporter gene expression after 24 hours. For the screen, we used HeLa-derived TZM-bl cells, which express endogenous CXCR4, transgenic CD4, and CCR5, and an integrated Tat-dependent β-galactosidase (β-Gal) reporter gene. The screen was optimized with siRNAs against Tat, CD4, and Rab9p40; Rab9p40 is required for HIV particle release (*5*). siRNAs targeting CD4 or Tat produced a more than threefold decrease in p24 expression (Fig. 1, B and C). Only modest protection was seen upon Rab9p40 depletion (Fig. 1C, part one). However, after incubation of fresh TZM-bl cells with transferred cultured supernatant, the depletion of Rab9p40 scored convincingly (Fig. 1C, part two).

This platform was used for a genome-wide screen. The siRNA library contains 21,121 pools of four siRNAs per gene. Pools were classified as hits if they decreased the percentage of p24-positive cells or β-Gal activity by ≥2 SDs from the plate mean [table S2, column E (*4*)]. We also required that the siRNAs did not decrease viable cells by >2 SDs. These criteria were met by 386 pools (1.8%). We next rescreened the four siRNAs from each pool separately. In this validation screen, 273 pools (71%) were confirmed with at least one siRNA scoring in either part one or two. There was a strong correlation between parts one and two. Only 28 genes appeared specifically in part two, suggesting that these factors act in late stages of infection (table S2, SOM Text).

HDF bioinformatics analysis. Of the confirmed HDFs, we identified 36 host factors (13%) previously implicated in HIV pathogenesis (table S1), including CD4, CXCR4, NMT1, Rab9p40, and components of the NF-κB and CREB transactivation pathways. Among the 237 remaining genes, more than 100 had two or more individual siRNAs score, reducing the likelihood of off-target effects (table S2). Subcellular localization, gene ontology (GO) biological processes, and molecular functions of the candidates are shown (Fig. 1, D and E; fig. S1, A and B; and table S3). One hundred and thirty-six GO biological process terms, assigned to 103 genes, were significantly enriched. Analysis of GO molecular functions identified enrichment for 17 nonredundant statistically significant terms assigned to 86 genes.

Several macromolecular complexes were also detected. The nuclear pore complex (NPC) Nup160 subcomplex had four of six subunits identified (Nup85, Nup107, Nup133, and Nup160). Because Nup160 subcomplexes are NPC scaffolds, their loss may impede HIV nuclear access (*6*). Depletion of components of Mediator (Med4, Med6, Med7, Med14, and Med28), which directly couples transcription factors to RNA polymerase II (Pol II) (*7*), inhibited infection, perhaps shedding light on the requirements for activators that bind the viral long terminal repeat (LTR). Two endoplasmic reticulum (ER)–Golgi–associated assemblages, the conserved oligomeric Golgi (COG) complex (*8*), and the transport protein particle (TRAPP) I complex (*9*), also scored with multiple components, perhaps due to HIV's dependency on transmembrane glycoproteins for nuclear entry. Three of the late-acting HDFs found in part two, OST48, STT3A and DPM1, encode enzymes involved in glycosylation (*10*, *11*). HIV Env requires glycosylation to be infectious (*12*). Early studies showed that glycosylation inhibitors prevent Env modification and blocked HIV fusion (*13*, *14*).

Among the unexpected associations was autophagy, a process essential for the degradation and recycling of cellular components. Targeted substrates are encapsulated in membrane-bound autophagosomes by two protein conjugation pathways (*15*). HIV infection depended on the presence of members of both pathways [Atg7, Atg8 (GABARAPL2), Atg12, and Atg16L2]. In addition, lysosomal-associated

[1]Department of Genetics, Center for Genetics and Genomics, Brigham and Women's Hospital, Howard Hughes Medical Institute, Harvard Medical School, Boston, MA 02115, USA. [2]Gastrointestinal Unit, Massachusetts General Hospital, Harvard Medical School, Boston, MA 02114, USA. [3]Immune Disease Institute and Department of Pediatrics, Harvard Medical School, Boston, MA 02115, USA. [4]Center for Computational and Integrative Biology, Harvard Medical School, Boston, MA 02114, USA. [5]Dana-Farber Cancer Institute, Division of AIDS, Harvard Medical School, Boston, MA 02115, USA.

*These authors contributed equally to this work.
†To whom correspondence should be addressed. E-mail: selledge@genetics.med.harvard.edu

HDFs (CLN3, and LapTM5) may also be required for autophagy.

HeLa cells are not the natural host for HIV. We wondered whether HDFs showed an expression bias in other cell types that might explain HIV tropism. We assessed the expression of 239 genes that were expressed in at least one of the 79 tissues in the Genomic Institute of the Novartis Research Fund (GNF) data set and found that 79 of 239 (33%) were enriched for high expression in immune cells [$P < 0.001$, top 7% expression; Fig. 1F and table S3 (*4*)].

HIV entry requires retrograde vesicular transport. Rab6A regulates retrograde Golgi transport and is important for recycling of Golgi-resident enzymes (*16*, *17*). Three of four siRNAs were confirmed in the validation round for both Rab6A and Rab6A′, which differ by three amino acids due to alternative splicing (table S2) (*16*). Rab6A′ controls endosomal trafficking and is the homolog of the yeast Ypt6

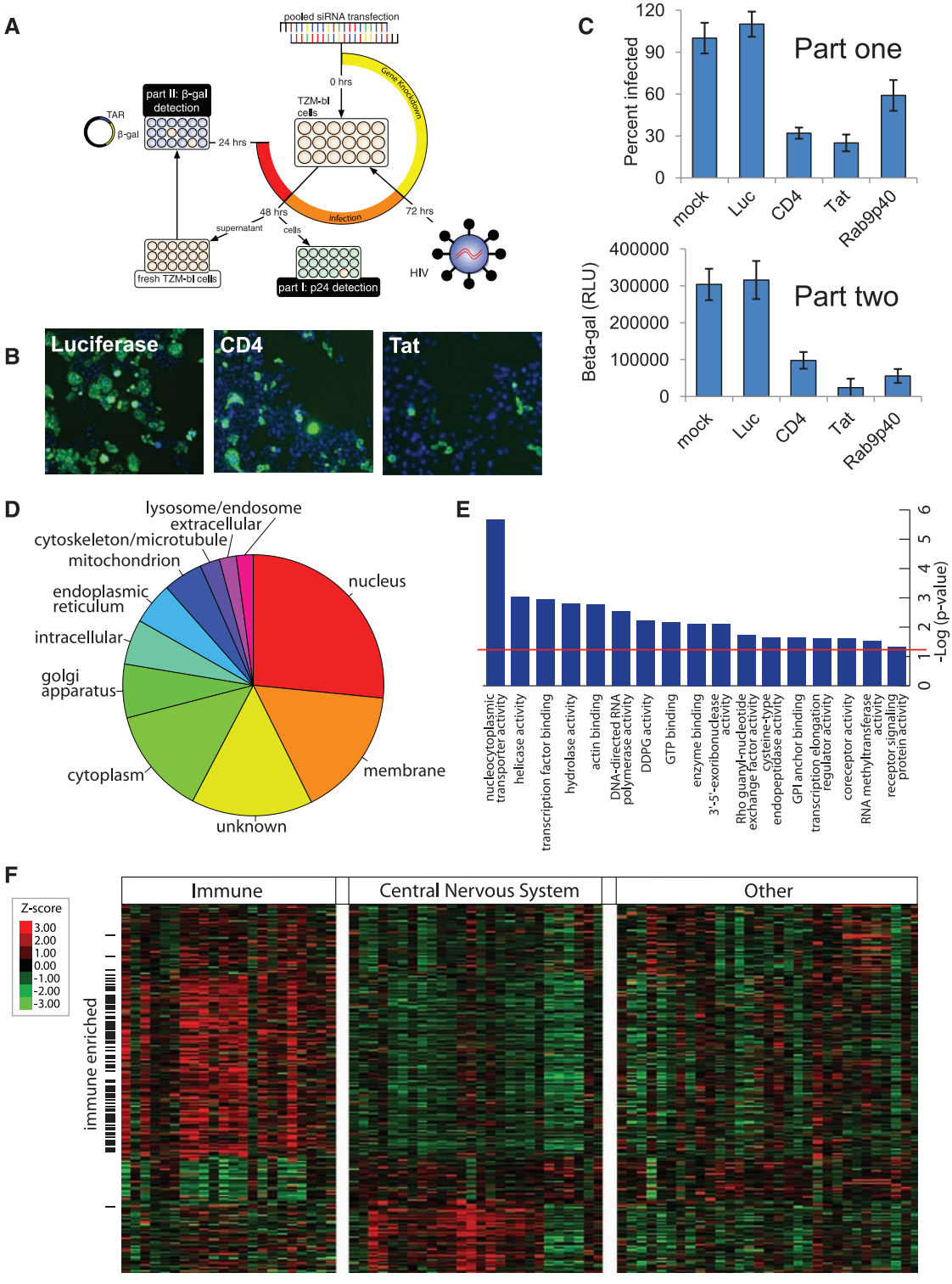

Fig. 1. siRNA screen for HDFs required for HIV infection with bioinformatics analyses. (**A**) Schematic representation of the screen. Arrayed pools of siRNAs were transfected into TZM-bl cells in a 384-well format. After 72 hours, HIV-IIIB virus was added, and 48 hours after infection, cultured supernatant was removed and added to fresh TZM-bl cells. In part one, 48 hours after infection, the siRNA transfected cells were fixed, permeabilized, stained, and imaged for HIV p24 protein and DNA. In part two, cells were cultured for 24 hours after the addition of supernatant, then lysed, exposed to a luminescent β-Gal substrate, and relative light units (RLU) recorded. (**B**) siRNAs against CD4 or Tat inhibit HIV infection (green: HIV p24; blue: cell nuclei). Magnification, ×4. (**C**) Screen part one measuring p24 staining, and part two measuring infectious virus production with the indicated siRNAs. (Percent infected is relative to control throughout.) Values represent the mean ± SD, $N \geq 4$. (**D**) Subcellular localization. Genes were manually curated on the basis of subcellular localization annotated in UniProt and GO. The localization for each protein is provided in table S3. (**E**) Molecular function analysis. The significance threshold is indicated by a red line at 1.3 = –log ($P = 0.05$). DDPG, dolichyl-diphosphooligosaccharide-protein glycotransferase; GPI, glycosylphosphatidylinositol. (**F**) Expression profiles across 79 tissues (in duplicate) of 239 HDFs. Expression values for each probe set were *Z*-score–transformed across all arrays (table S3). Of the 239 probes in duplicate in GNF, 79 probes were significantly ($P < 0.05$) higher when expressed in immune tissues compared to all other tissues and are indicated by black bars on the left. Gene names and *P*-values are provided in table S3.

(*16*); both isoforms will hence be referred to as Rab6. Ypt6 mutants are defective in retrograde Golgi transport, particularly recycling of glycosyltransferases (*17*, *18*). Depletion of the homolog of Rgp1p, a guanine nucleotide exchange factor required for Ypt6 function, also decreased HIV infection [table S2 (*19*)].

We generated cells stably expressing short hairpin RNA (shRNAs) directed against Rab6. All three shRNAs decreased infection proportional to Rab6 depletion (Fig. 2, A to C) in the first phase of the life cycle because Rab6 depletion inhibited Tat-dependent reporter expression 20 hours after infection (Fig. 2B). Expression of Rab6-GFP (green fluorescent protein) lacking the Rab6 3′-untranslated region targeted by the shRNAs rescued susceptibility to infection (Fig. 2, A to C, and fig. S2). Given Rab6's role in vesicular transport, we examined surface expression of CD4 and CXCR4 by fluorescence-activated cell sorting (FACS) in the Rab6 knockdown (Rab6-KD) lines. CXCR4 expression showed minor variations that did not correlate with resistance to HIV or Rab6 depletion and were not restored upon Rab6 repletion (fig. S3, A and B). CD4 levels were unaltered (fig. S3C). Thus, something other than receptor expression is defective in Rab6-KD cells.

To characterize the block to infection further, we infected Rab6-KD cells with either HIV-IIIB or an HIV strain pseudotyped with the vesicular stomatitis virus G envelope protein (VSV-G), containing a yellow fluorescent protein (YFP) reporter in place of *nef* (HIV-YFP). Only HIV-IIIB infection was inhibited (Fig. 2D). In addition, VSV-G–pseudotyped Moloney leukemia virus–enhanced GFP (MLV-EGFP) infection was unperturbed. HIV envelope proteins promote fusion of the virus to the cell membrane. In contrast, VSV-G pseudotypes are endocytosed, with endosomal acidification triggering fusion. Thus, our initial observations suggested that Rab6 acted early in infection. HIV-IIIB has tropism for the co-receptor CXCR4. To determine whether inhibition was restricted to CXCR4 virus, we examined the effect of Rab6 silencing on infection with HIV-Bal, a CCR5-tropic virus. Targeting Rab6 did not alter surface CCR5 expression (fig. S3G), but did inhibit HIV-Bal infection (Fig. 2E). Therefore, Rab6 plays a role in infection by both CCR5 and CXCR4 viruses.

Rab6 was required for late reverse transcription of the viral genome, indicating an early block (Fig. 2F). We therefore tested Rab6's role in fusion by coculturing HL2/3 HeLa cells, which express Tat and HIV receptor proteins gp41 and gp120, with TZM-bl cells. HL2/3 viral receptors interact with CD4 and CXCR4 on TZM-bl cells, prompting cellular fusion via the same mechanism used by HIV. Upon fusion, Tat activates β-Gal expression. Decreased Rab6 levels correlated with diminished β-Gal activity, consistent with inhibition of viral fusion [Fig. 2G and fig. S4C (*4*)]. To test Rab6's role in HIV infection in a more physiologic cell, we trans-

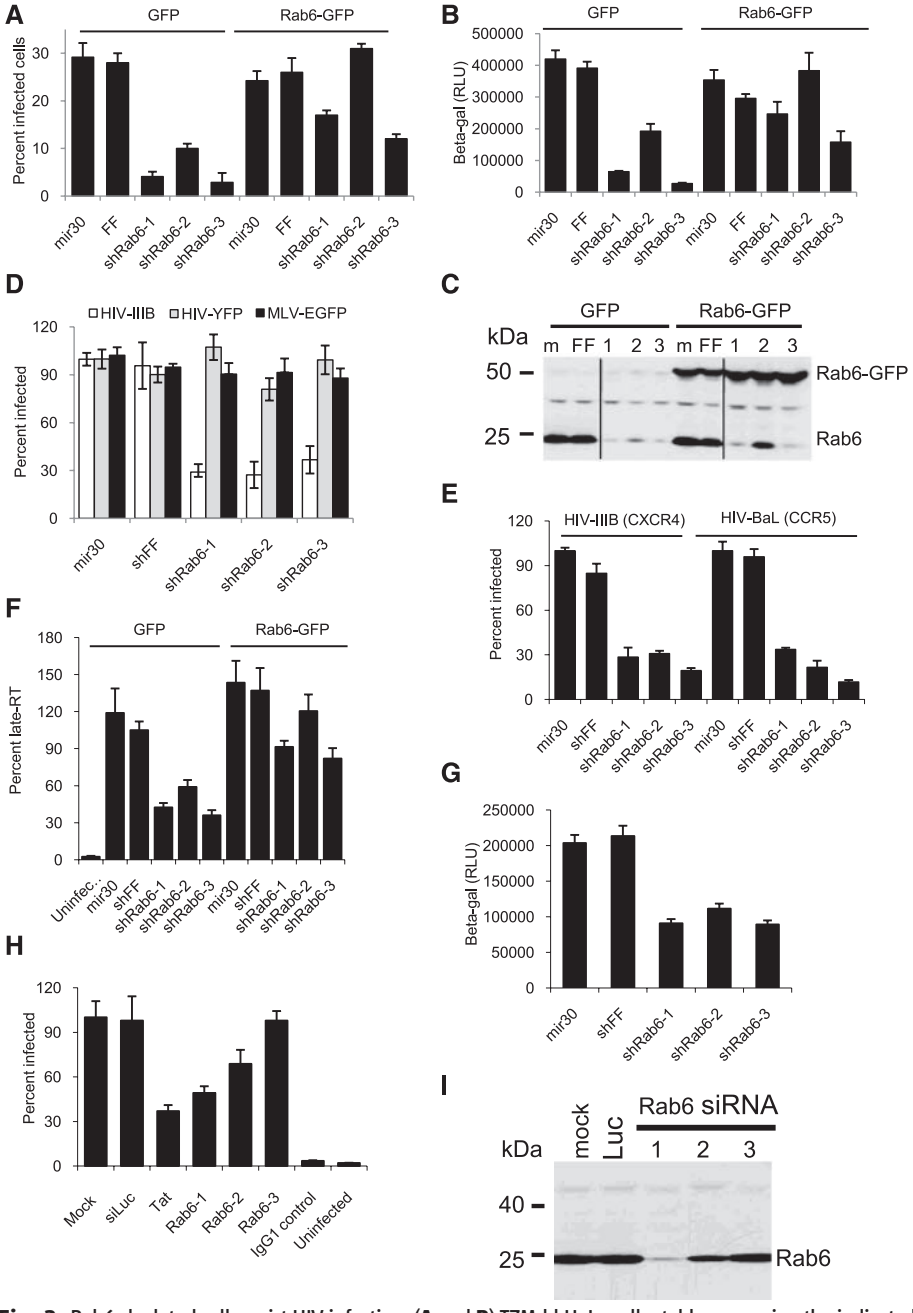

Fig. 2. Rab6-depleted cells resist HIV infection. (**A** and **B**) TZM-bl HeLa cells stably expressing the indicated shRNAs, and either the control green fluorescence protein (GFP) or a Rab6-GFP fusion (Rab6-GFP), were infected with HIV-IIIB and analyzed for (A) p24 at 48 hours after infection or (B) Tat-dependent β-Gal expression at 20 hours after infection. Empty vector (mir30), firefly luciferase (FF), shRNAs against Rab6 (shRab6-1, 2, and 3). Values represent the mean ± SD, $N \geq 3$. (**C**) Western blots for Rab6 and Rab6-GFP levels for cells shown in (A) and (B). (**D**) Rab6 depletion specifically inhibits WT-enveloped HIV. The indicated cell lines were infected with either HIV-IIIB, VSV-G pseudotyped HIV-YFP, or MLV-EGFP. Infection was monitored by immunofluorescence (IF) of p24 (HIV-IIIB) or the reporter genes (EGFP, YFP) at 48 hours after infection. Percent infected cells is relative to control throughout. (**E**) HIV infection via either the CXCR4 or CCR5 co-receptor is attenuated by Rab6 depletion. Cells were infected with either HIV-IIIB or HIV-Bal and p24 stained at 48 hours after infection. (**F**) Rab6 depletion blocks HIV before late reverse transcription. Cell lines indicated were infected with HIV-IIIB, and the late reverse transcription products (late RT) were assessed by qPCR. Percent late-RT product is relative to control. (**G**) Rab6 loss inhibits cell fusion. The indicated TZM-bl cell lines containing a Tat-dependent β-Gal reporter were layered for 6 hours with HL2/3 cells expressing HIV-1 Env and Tat proteins. The relative amount of cell fusion was quantified by assaying β-Gal activity. (**H**) Rab6 depletion protects T cells from HIV. Jurkat cells were transfected with the indicated siRNAs for 72 hours, then infected with HIV and analyzed by FACS with antibodies to either p24 (anti-p24) or an isotype matched control (immunoglobulin G1, IgG1) antibody at 48 hours after infection. (**I**) Cells from (H) were examined for Rab6 protein by Western blotting.

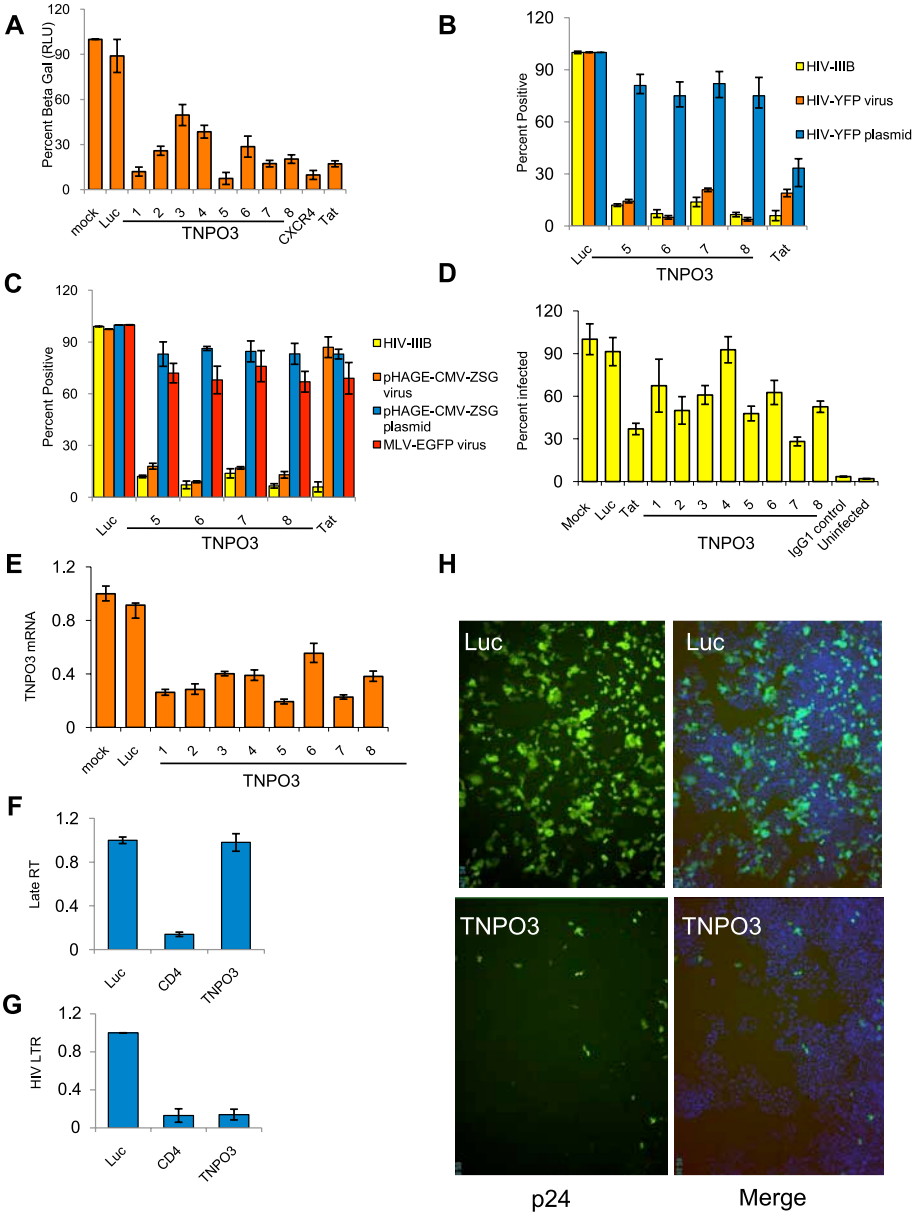

Fig. 3. TNPO3 is required for HIV infection. (**A**) Cells were transfected with the indicated siRNAs for 72 hours, then infected with HIV-IIIB. After 20 hours, β-Gal activity was measured. Values represent the mean ± SD, $N \geq 3$ throughout. (**B**) Cells were transfected with the indicated siRNAs for 72 hours, then infected with either HIV-IIIB or pseudotyped HIV-YFP, or transfected with the HIV-YFP plasmid. After 48 hours, the percentage of positive cells was determined by p24 (HIV-IIIB) or YFP expression (HIV-YFP virus and plasmid). (**C**) TNPO3 depletion preferentially affects lentiviruses. TZM-bl cells were transfected with the indicated siRNAs for 72 hours, then infected with the indicated viruses or transfected with the Tat-independent pHAGE-CMV-ZSG plasmid. After 48 hours, levels of p24, ZSG, or EGFP were measured. (**D**) TNPO3 depletion protects T cells from HIV. Jurkat cells were transfected with the indicated siRNAs for 72 hours, then infected with HIV-IIIB and analyzed by FACS with either anti-p24 or an isotype control antibody at 48 hours after infection. (**E**) TNPO3 mRNA reduction by siRNAs. TZM-bl cells were transfected with the indicated siRNAs for 72 hours, then cDNA was prepared and TNPO3 expression levels were measured by qPCR. (**F** and **G**) TNPO3 depletion inhibits HIV after reverse transcription, but before integration. TZM-bl cells were transfected with the indicated siRNAs (TNPO3, siRNAs 5 to 8 pooled) and infected with HIV 72 hours later. Late RT levels were assessed by qPCR, and integrated viral DNA (HIV LTR) was quantified by nested Alu-PCR. (**H**) IF images showing the block to HIV infection with loss of TNPO3. Cells were treated as described in (B), with either the luciferase (Luc), negative control siRNA; or TNPO3, siRNA #8 targeting TNPO3. "Merge" denotes the combined image for nuclei (blue) and HIV p24 (green).

fected a T cell line, Jurkat, with Rab6 siRNAs, then infected the cells with HIV. Reduced infection was seen after transfection with two of three Rab6 siRNAs tested (Fig. 2H), correlating with Rab6 depletion (Fig. 2I). No effect on receptor levels was observed in the transfected T cells (fig. S3, E and F).

Similar results were obtained for Vps53 (figs. S4, A to F, and S5). Yeast Vps53 is a component of the Golgi-associated retrograde protein (GARP) complex. GARP targets transport vesicles trafficking from endosomes to the trans-Golgi network in a Ypt6-dependent manner (*20*–*23*). Together, these data suggest that retrograde vesicular trafficking is needed for HIV infection, possibly at viral entry.

A role for a karyopherin in HIV replication. Transportin 3 (TNPO3), a karyopherin, imports multiple proteins into the nucleus, including histone mRNA stem-loop binding protein [SLBP (*24*)], serine/arginine-rich proteins (SR proteins) that regulate splicing of mRNA (*25*), and repressor of splicing factor [RSF1 (*26*)]. Eight of eight TNPO3 siRNAs lowered infection in HeLa cells (Fig. 3, A and H). TNPO3 mRNA reduction, as determined by quantitative polymerase chain reaction (qPCR), correlated with the inhibition of infection (Fig. 3E). Prevention of infection by TNPO3 silencing was independent of HIV envelope (Fig. 3B). TNPO3 depletion also inhibited infection of Jurkat cells (Fig. 3D).

TNPO3 depletion did not significantly affect MLV-EGFP (Fig. 3C). This could be explained if TNPO3 depletion impaired SR protein–dependent splicing of Tat, which is required for efficient HIV, but not γ-retroviral, transcription. However, Tat-dependent reporter gene expression from a transiently transfected HIV-YFP plasmid was only weakly affected by TNPO3 depletion (Fig. 3B). Additionally, an HIV derivative, pHAGE-CMV-ZSG, that contains HIV Gag and Pol, but expresses a fluorescent reporter protein from an internal CMV promoter, also showed a dependency on TNPO3 upon viral infection, but not plasmid transfection (Fig. 3C).

These observations suggest that TNPO3 is needed before viral mRNA splicing. Assays for late RT products and integrated viral DNA in TNPO3-depleted cells showed that the block occurred after reverse transcription but before integration (Fig. 3, F and G). Thus, diminished TNPO3 produces a lentiviral-specific preintegration block, perhaps at the stage of PIC nuclear import. Whether TNPO3 directly interacts with the virus or indirectly, via altered import or splicing of an HDF required for integration, remains to be determined.

The Mediator complex in HIV infection. Depletion of several components of Mediator inhibited HIV infection. We focused on Med28 because all four Med28 siRNAs inhibited first-round HIV infection (Fig. 4A and fig. S6). Med28 depletion also protected Jurkat cells and

efficiently decreased target gene protein levels (Fig. 4, C and D). Loss of Med28 appeared to specifically affect HIV because it inhibited both HIV-IIIB and HIV-YFP, but not MLV (Fig. 4B). We found no decreases in reverse-transcribed cDNA or integrated proviral DNA upon Med28 depletion (Fig. 4, E and F). However, Med28 loss also decreased YFP expression from a transiently transfected HIV-YFP plasmid (Fig. 4G). Therefore, we conclude that Med28 is required for transcription of viral genes, consistent with its connection to RNA Pol II.

Discussion. Judging from the diverse cellular processes detected in our screen, the exploitation of host cell functions by HIV is extensive. The functional clustering and confirmation of HDFs provide internal validation for our screen and suggest that most of the 237 proteins identified with no previous links to HIV are likely to play relevant roles in HIV pathogenesis. We have portrayed the HIV viral life cycle along with the presumed subcellular locations and functions of the novel and known HDFs in Fig. 5 [rationale provided in table S4 (*4*)].

Additional validation comes from the analysis of the enrichment of genes connected to known proteins implicated in HIV function. We find a strong enrichment for connectivity to this data set [fig. S7 and table S5 (*4*)]. Furthermore, although the screen was performed in HeLa cells, one-third of the confirmed HDFs were significantly enriched for high expression in immune cells. This suggests that immune cells are especially proficient for the functions HIV needs for optimal replication and became the selected host for that reason. It will be interesting to determine if the virus is especially reliant on this set of proteins and whether the tropism of other viruses can be similarly explained.

Rab6 and Vps53 are required for viral fusion to the membrane through an unknown mechanism. Although we have ruled out alteration of host co-receptor cell surface expression, several alternative explanations exist. There could exist a previously undetected co-receptor, dependent on Rab6 and Vps53. The screen identified more than 30 transmembrane proteins with no known HIV association (table S2). Modification of host receptors may be aberrant. However, no modification of either CD4 or CXCR4 is known to be required for infection (*27*, *28*). Alternatively, the plasma membrane composition may be affected, possibly due to alterations in the major supplier of membrane, the Golgi. Among the candidates affected by such a perturbation are the glycosphingolipids (GSLs), which are required for HIV-host cell fusion (*29*–*31*). GSLs are synthesized by ER and Golgi enzymes (*32*) that depend on retrograde vesicular transport for recycling (*18*, *33*). Rab6/Ypt6 mutants are defective in retrograde Golgi transport, resulting in vesicular scattering and lysosomal degradation of many Golgi resident enzymes, possibly altering GSL homeostasis (*18*, *20*) (SOM Text).

The HIV PIC accesses our genome through the NPC. A candidate for the PIC-associated karyopherin is TNPO3, depletion of which profoundly blocked provirus formation. This effect might be indirect if TPNO3 is required for the activity of another HDF. However, a simpler model involves the PIC binding to TNPO3, then entering the nucleus via interactions with two NPC proteins detected in the screen, RanBP2 and Nup153 (*34*). Although speculative, these are examples of the kinds of detailed hypotheses that can be generated from a highly validated, functionally derived data set.

A key pharmacological strategy for treating individuals living with HIV has been to simultaneously target multiple virus-encoded enzymes required for replication to overcome emergence of drug resistance. We have taken a parallel strategy by identifying host factors required for the HIV life cycle. Such proteins represent therapeutic targets that are not plagued by the twin problems of viral diversity and escape mutation that interfere with the effectiveness of conventional antiretroviral drugs. We anticipate that HIV would be hard-pressed to evolve resistance to drugs targeting cellular proteins, because it would have to evolve a new capability, not simply mutate a drug-binding site. This is analogous to blocking angiogenesis in nontumor cells to deprive cancer of a blood supply (*35*). Support for the notion that these HDFs may represent potential therapeutic targets arises in part from a recent genome association study reporting that single-nucleotide polymorphisms in ZNRD1 are associated with slowed HIV disease progression (*36*). Our screen found that ZNRD1 depletion inhibited HIV (table S2). This suggests that variants in other HDFs might modulate HIV in-

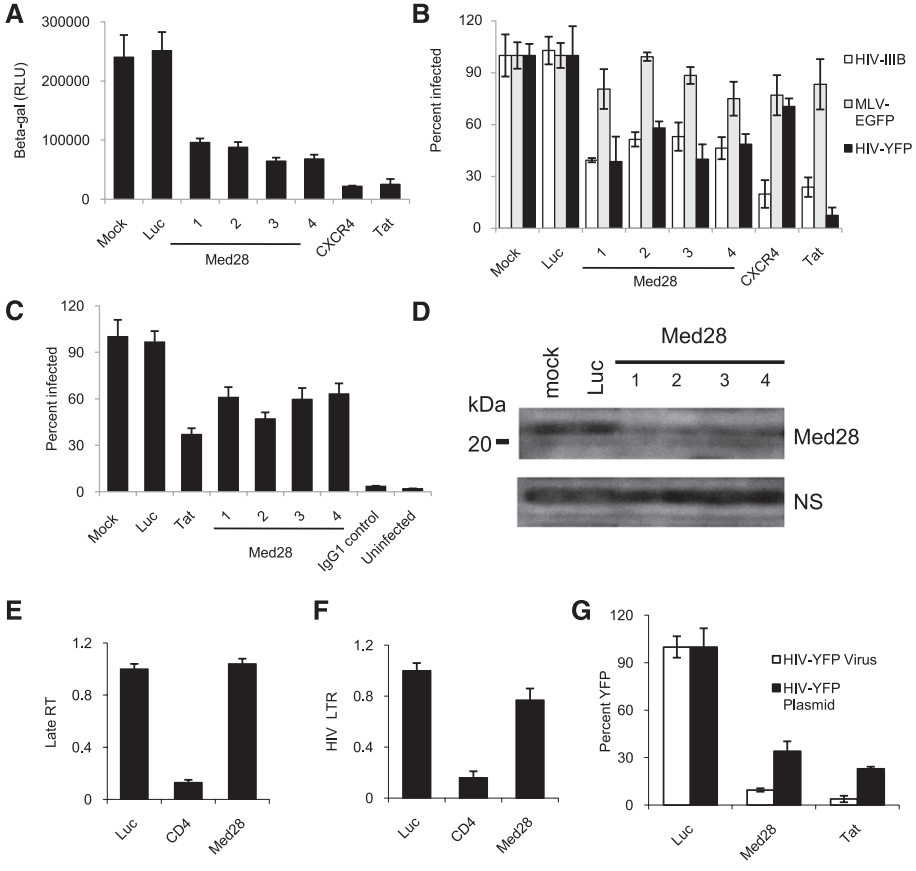

Fig. 4. Med28 silencing inhibits HIV replication. (**A**) Cells were transfected with the indicated siRNAs for 72 hours, then infected with HIV-IIIB. After 20 hours, β-Gal activity was measured. Values represent the mean ± SD, $N \geq 3$, throughout. (**B**) Loss of Med28 inhibits WT-enveloped and VSV-G–pseudotyped HIV. TZM-bl cells were transfected with the indicated siRNAs, and then infected with the indicated viruses 72 hours after transfection. Infection was monitored by IF staining for p24 or reporter expression 48 hours after infection. (**C** and **D**) Med28 depletion protects T cells from HIV. Jurkat cells were transfected with the indicated siRNAs for 72 hours, then infected with HIV and analyzed by FACS with either anti-p24 or an isotype antibody control at 48 hours after infection. Jurkat cells from these cultures were also assessed for Med28 protein by Western blotting (D); NS, nonspecific band. (**E** and **F**) Med28 depletion inhibits HIV transcription. TZM-bl cells were transfected with the indicated siRNAs (Med28, siRNAs 1 to 4 pooled) and infected with HIV 72 hours later. Late RT product levels were assessed by qPCR (E), and integrated viral DNA (HIV LTR) was quantitated by nested Alu-PCR (F). (**G**) TZM-bl cells were transfected with the indicated siRNA pools for 72 hours, then infected with HIV-YFP virus or transfected with HIV-YFP plasmid. Levels of YFP reporter protein were monitored by IF 48 hours later.

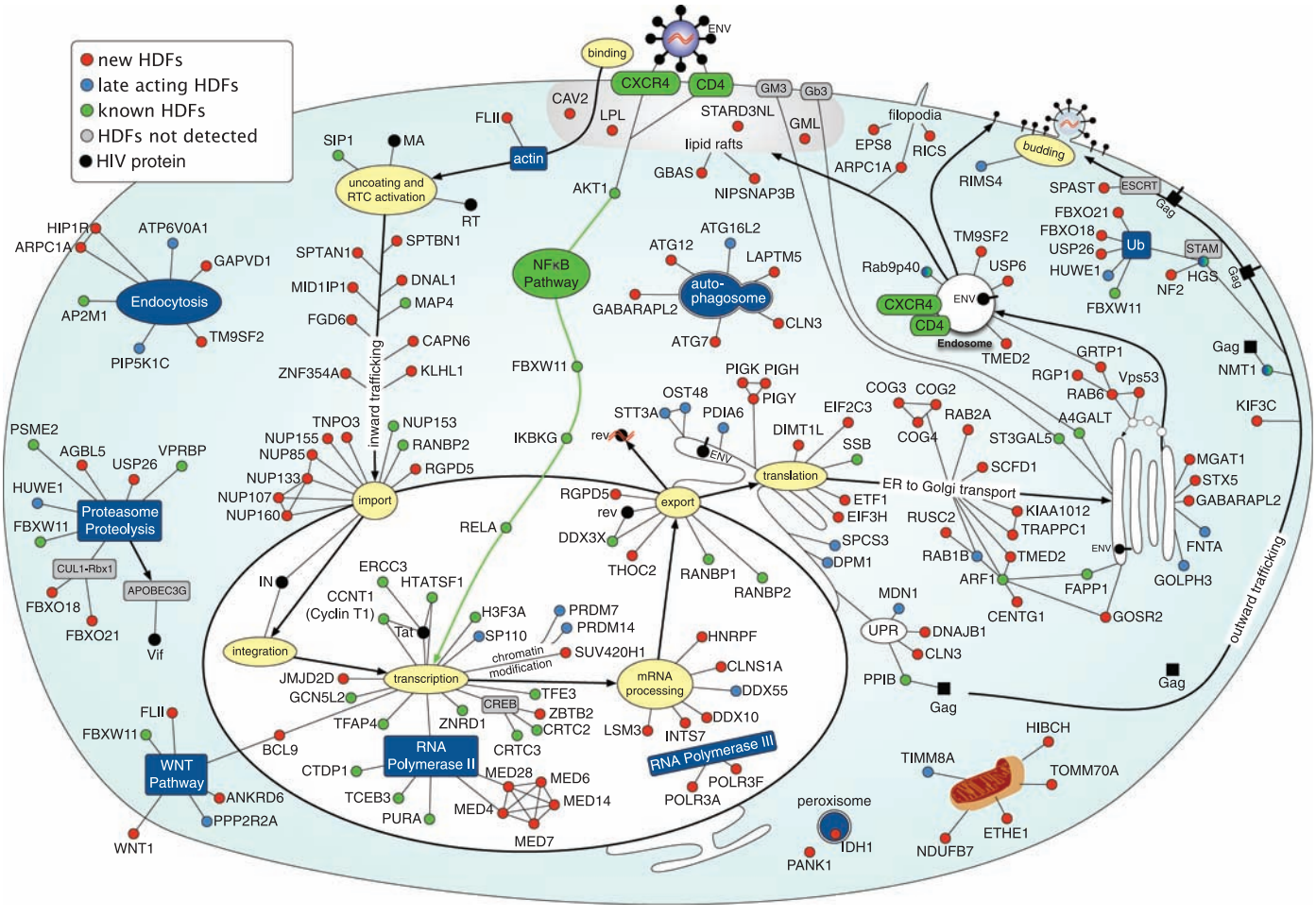

Fig. 5. Model of HDF roles in the HIV life cycle. With the stages of the HIV life cycle as a framework, each HDF was placed at the position most likely to elicit HIV dependency. The function and subcellular location of HDFs were determined with the use of multiple databases (rationale, table S4). Some proteins are in multiple locations to represent more than one possible role in the HIV life cycle. Newly identified HDFs (red or blue, the latter if they inhibited HIV in part two only); previously implicated HDFs detected in the screen (green), or not detected but with a relevant interaction (gray); HIV protein (black): matrix (MA), reverse transcriptase (RT), integrase (IN), envelope (gp41, gp120) (ENV). Unfolded protein response, UPR.

fection, and drugs inhibiting their functions may prove protective.

References and Notes

1. A. D. Frankel, J. A. Young, *Annu. Rev. Biochem.* **67**, 1 (1998).
2. S. P. Goff, *Nat. Rev. Microbiol.* **5**, 253 (2007).
3. E. Morita, W. I. Sundquist, *Annu. Rev. Cell Dev. Biol.* **20**, 395 (2004).
4. Materials and methods are available as supporting material on *Science* Online.
5. J. L. Murray *et al.*, *J. Virol.* **79**, 11742 (2005).
6. A. Harel *et al.*, *Mol. Cell* **11**, 853 (2003).
7. R. D. Kornberg, *Trends Biochem. Sci.* **30**, 235 (2005).
8. D. Ungar, T. Oka, M. Krieger, F. M. Hughson, *Trends Cell Biol.* **16**, 113 (2006).
9. Y. G. Kim *et al.*, *Cell* **127**, 817 (2006).
10. H. Ashida, Y. Maeda, T. Kinoshita, *J. Biol. Chem.* **281**, 896 (2006).
11. D. J. Kelleher, R. Gilmore, *Glycobiology* **16**, 47R (2006).
12. T. Wolk, M. Schreiber, *Med. Microbiol. Immunol. (Berl.)* **195**, 165 (2006).
13. H. A. Blough *et al.*, *Biochem. Biophys. Res. Commun.* **141**, 33 (1986).
14. J. Balzarini, *Nat. Rev. Microbiol.* **5**, 583 (2007).
15. N. Mizushima, *Genes Dev.* **21**, 2861 (2007).
16. E. Del Nery *et al.*, *Traffic* **7**, 394 (2006).
17. A. Girod *et al.*, *Nat. Cell Biol.* **1**, 423 (1999).
18. Z. Luo, D. Gallwitz, *J. Biol. Chem.* **278**, 791 (2003).
19. S. Siniossoglou, S. Y. Peak-Chew, H. R. Pelham, *EMBO J.* **19**, 4885 (2000).
20. E. Conibear, T. H. Stevens, *Mol. Biol. Cell* **11**, 305 (2000).
21. N. R. Quenneville, T. Y. Chao, J. M. McCaffery, E. Conibear, *Mol. Biol. Cell* **17**, 1859 (2006).
22. S. Siniossoglou, H. R. Pelham, *EMBO J.* **20**, 5991 (2001).
23. S. Siniossoglou, H. R. Pelham, *J. Biol. Chem.* **277**, 48318 (2002).
24. J. A. Erkmann *et al.*, *Mol. Biol. Cell* **16**, 2960 (2005).
25. M. C. Lai, R. I. Lin, S. Y. Huang, C. W. Tsai, W. Y. Tarn, *J. Biol. Chem.* **275**, 7950 (2000).
26. E. Allemand, S. Dokudovskaya, R. Bordonne, J. Tazi, *Mol. Biol. Cell* **13**, 2436 (2002).
27. D. J. Chabot, H. Chen, D. S. Dimitrov, C. C. Broder, *J. Virol.* **74**, 4404 (2000).
28. J. Wang *et al.*, *Virology* **324**, 140 (2004).
29. P. Hug *et al.*, *J. Virol.* **74**, 6377 (2000).
30. A. Puri *et al.*, *AIDS* **18**, 849 (2004).
31. P. N. Nehete *et al.*, *Antiviral Res.* **56**, 233 (2002).
32. A. H. Futerman, H. Riezman, *Trends Cell Biol.* **15**, 312 (2005).
33. R. Conde, G. Pablo, R. Cueva, G. Larriba, *Yeast* **20**, 1189 (2003).
34. N. Sabri *et al.*, *J. Cell Biol.* **178**, 557 (2007).
35. J. Folkman, *Exp. Cell Res.* **312**, 594 (2006).
36. J. Fellay *et al.*, *Science* **317**, 944 (2007).

37. We thank the Institute of Chemistry and Cell Biology (ICCB)-Longwood: C. Shamu, S. Rudnicki, S. Johnston, D. Fletcher, K. Schulberg, and M. Tsui. We also thank F. Diaz-Griffero, J. Walsh, A. Balazs, R. Mulligan, R. Sutton, V. Ramesh, and A. Puri for reagents and guidance; B. Glick, G. Hu, E. R. McDonald III, A. Smorgorzewska, N. Solimini, M. Krishnan, and members of the Elledge lab for help and advice; A. Liao, A. Landry, and Z. Wu for technical assistance; and E. Golde for facilitating collaborations. Funding for this study was provided by a Crohns and Colitis Foundation of America fellowship (A.L.B.), a Center for Computational and Integrative Biology fellowship (Y.B.), and the Harvard Center for AIDS Research (CFAR) scholar award (N.Y.). J.L. (U19-AI056900), R.J.X. (AI062773), and A.E. (AI052014) are supported by NIH grants. D.M.D. was funded by a grant from the Harvard CFAR to J.L. and S.J.E. S.J.E. is an Investigator with the Howard Hughes Medical Institute.

Supporting Online Material

www.sciencemag.org/cgi/content/full/1152725/DC1
Material and Methods
SOM Text
Figs. S1 to S7
Tables S1 to S5
References

7 November 2007; accepted 21 December 2007
Published online 10 January 2008;
10.1126/science.1152725
Include this information when citing this paper.